Development of Computed Tomography Head and Body Phantom for Organ Dosimetry

Michael Onoriode Akpochafor[1], Samuel Olaolu Adeneye[1], Ololade Kehinde[1], Akintayo Daniel Omojola[2], Ajibade Oluwafemi[1], Adedewe Nusirat[1], Adedokun Aderonke[1], Moses Adebayo Aweda[1], Oluyemi Bright Aboyewa[3]

1. Department of Radiation Biology, Radiotherapy, Radiodiagnosis and Radiography, Lagos Teaching Hospital, Faculty of Medicine, Idi-Araba, Lagos, Nigeria
2. Department of Radiology, Medical Physics Unit, Federal Medical Centre Asaba, Delta State, Nigeria
3. Department of Physics, Federal University of Technology, Akure, Ondo State, Nigeria

ARTICLE INFO	ABSTRACT
	Introduction: Quality assurance in Computed tomography (CT) centers in developing countries are largely hindered by the unavailability of CT phantoms. The development of a local CT phantom for the measurement of organ radiation absorbed dose is therefore requisite. *Material and Methods:* Local CT phantoms were designed to meet the standard criteria of 32 cm diameter for body, 16 cm diameter for head, and 14 cm in length respectively. The outer plastic shell was made using poly (methyl methacrylate [PMMA]) sheet. The developed CT phantoms were validated against a standard phantom. Radiation absorbed dose was determined by scanning the setup with the same protocol used for the standard phantom. The local phantoms were then verified for organ radiation absorbed dose measurement using bovine tissues. The set up was CT-scanned, and Hounsfield units (HU) for bovine tissues were obtained. *Results:* There was no significant difference between the local and standard head phantoms (P=0.060). Similarly, no difference was noted between the local and standard body phantoms (P=0.795). The percentage difference in volume CT dose index (CTDI$_{vol}$) between the body (local and standard) phantoms was higher than that for the head phantoms. There were no significant differences in HU between bovine and human brain, liver, kidney and lung tissues (P=0.938). *Conclusion:* The local phantoms showed good agreement with the standard ones. The developed phantoms can be used for CT organ radiation absorbed dose measurement in radiology departments in Nigeria.

Introduction

Diagnostic imaging modalities such as computed tomography (CT) are very useful for visualizing internal structures. They can generate images in different planes of the human anatomy by reconstructing X-ray attenuation through the tissues into 2D array of pixels (picture elements) and 3D voxels (volume elements) [1]. Unlike conventional radiography and mammography, radiation doses are higher in CT due to its high scan parameters [2]. Therefore, increased use of CT facilities elevates radiation doses to the staff and population, which justifies continuous efforts in dose reduction [3]. The risks associated with CT procedures may be deterministic or stochastic [4]. To minimize or avoid these effects, there is a need to optimize patient dose while still achieving satisfactory image quality [5]. Several parameters can be used to explain CT dose over a region, namely volume CT dose index (CTDI), Dose Length Product (DLP), and effective dose (E). Different outcomes of the above parameters are mainly due to scanner type, model, operator parameters, and body size [6-10].

There are two methods of measuring specific organ doses; firstly, by virtual stimulation or indirect measurements using special computer software (e.g., CT-EXPO, CT DOSE, Impact Dose, and Virtual Dose), and secondly, by direct or experimental measurements with phantoms and detectors. The direct evaluation of organ doses is performed on the patient or an anthropomorphic phantom using radiation dosimeters such as ionization chamber or smaller devices like thermo-luminescence detectors (TLD), optically stimulated luminescence (OSL), and photodiode dosimeters.

Corresponding Author: Tel: +2348137850394; Email: akpochafor@gmail.com

Phantoms are mimicked materials with almost the same electron density as human tissues or organs. Usually, their HUs are close to those of real human body, and they have the capacity to yield results close to an actual scan; an example is the Rando Alderson phantom.

Two standard body regions are usually used for measurement, which are the 16-cm head and the 32-cm body phantoms made of Plexiglas. It was recommended by the American Association of Physicists in Medicine (AAPM) for CT vendors to perform measurement with 16 cm diameter head and 32 cm diameter body phantoms with a length of 14 cm, which are considered the standard methods [11]. Every quality control CT phantom has five inserts, including the ionization chamber port. Measurements are made in the air, center, and peripheries (i.e., 12, 3, 6, and 9 o'clock) with a 100-mm ionization chamber. Most recent chambers can now estimate CTDI and DLP through a Digital Imaging and Communication in Medicine (DICOM) from the point of measurement to the control console.

CTDI is the integral of air-Kerma along the rotational symmetry axis for the X-ray tube (Z) divided by the number of simultaneously acquired slices (N) of nominal thickness (T):

$$\text{CTDI (mGy)} = \frac{1}{N.T} \int_{-L/2}^{+L/2} K(Z)dz \qquad (1)$$

Where L denotes the length over which the integral is made. Most often, the detector used is a pencil-shaped ionization chamber with an effective measuring length of 100 mm. This means that Equation 1 needs to be integrated from $-\frac{L}{2}$ = -50 mm to $+\frac{L}{2}$ = 50 mm, with the correct denotation as CTDI_{100} [12, 13]. Dose measured at the center and the peripheral can be combined to give a single estimate, i.e. a weighted CTDI_w, of the radiation dose to the phantom [14]:

$$\text{CTDI}_w = \frac{1}{3} . \text{CTDI}_{100;c} + \frac{2}{3} . \text{CTDI}_{100;p} \qquad (2)$$

Where $\text{CTDI}_{100;c}$ is the CTDI_{100} from the central hole and $\text{CTDI}_{100;p}$ is the average CTDI_{100} from the peripheral holes. Assuming a linear decrease of the air-Kerma in the CTDI phantoms from the periphery to the center, the factors $\frac{2}{3}$ and $\frac{1}{3}$ represent the relative air-Kerma contribution [15]. CTDI_w can be interpreted as the average air-Kerma in the irradiated cross section.

Another CTDI descriptor that takes into account any gaps between successive scanning or successive scanning without table translation is CTDI_{vol} (mGy), which is introduced below [13]:

$$CTDI = \begin{cases} \frac{NT}{\Delta d} . CTDI_w \ axial \ scanning \\ \frac{NT}{\Delta d} . CTDI_w = \frac{CTDI_w}{pitch} \ helical \ scanning \\ n_{tr} . CTDI_w \ without \ table \ translations \end{cases} [mGy] \quad (3)$$

Where N is the number of simultaneously acquired slices of nominal thickness (T). For axial sequential scanning, Δd is the table translation between consecutive scans. For helical scanning, Δd is the table translation for one tube rotation, and the ratio $\frac{\Delta d}{NT}$ denotes the pitch. A special case is when there is no table translation, then CTDI_{vol} is defined as the number of tube rotations (n_{tr}) multiplied by CTDI_w. When a patient is being CT-scanned, the scanning is performed over the length used for image reconstruction. In this case, the scanned length is slightly longer than the reconstructed length. To obtain a rendering of the whole radiation exposure across the total scanned length, the term DLP is introduced [13]:

$$DLP = \begin{cases} CTDI_{vol} . \Delta d . n_s \ axial \ scanning \\ CTDI_{vol} . L \ helical \ scanning \\ CTDI_{vol} . NT \ without \ table \ translations \end{cases} [mGy.cm] \quad (4)$$

Where for axial scanning, Δd is the table translation between the consecutive scans, and n_s is the number of scans in the series. For helical scanning, L is the total table translation during the series. In special cases where no table translation is carried out, length is defined as the number of simultaneously acquired slices (N) of nominal thickness (T).

Commercial phantoms developed for dosimetric studies in CT (quality assurance [QA] and quality control [QC]) are very costly and rarely available in the developing countries like Nigeria due to the high cost. For example, only one phantom is currently available at the National Hospital, Abuja. This prompted the need to develop a cheap, purpose-built local phantom.

Materials and Methods

Local CT phantoms were designed to meet the standard criteria of 14 cm in length and 16 cm diameter head and 32 cm diameter body scans. The outer plastic shell was produced using poly (methyl methacrylate [PMMA]) sheet bent to give the desired spherical shape. The PMMA or acrylic sheet is a transparent plastic, which is lightweight for easy mobility and has a density of 1.185 g/cm^3, with a thickness of 3 mm. The inserts were made using five closed-end acrylic tubes with a thickness of 2.3 mm and length of 10 cm. Four of the tubes were placed in holes drilled at the periphery, 1 cm away from the edges of the outer shell with the fifth at the center. Also, an inlet was made for water. Gas was used to supply heat for softening of the plastics for easy malleability. The arrangement was fitted together permanently with a local gum as shown in Figure 1. A standard/commercial CT phantom for dosimetry was used for the validation of the local CT phantoms (head and body). TLD100: LiF:Mg,Ti (Fimel, France), was used for this study. Three of the TLDs were placed in between a Styrofoam at the central insert of the

phantoms (standard and local). The phantoms were filled with water for air attenuation correction and uniformity (homogeneity) and imaged in the CT device (Aquilion – CXL, Toshiba, Japan) as shown in Figure 2. The local and standard phantoms were scanned with the same protocol as in Table 1. The CTDI was obtained from the CT console and the TLDs (Rados RE2000 Mirion Technologies, USA). The readings from the developed phantoms were then compared to those of the standard phantoms using the formula:

$$\% \text{ Deviation} = \frac{(D_{meas} - D_{ref})}{D_{ref}} \times 100 \qquad (5)$$

where D_{meas} is the measured dose (TLDs reading or CTDI) using the local phantom, and D_{ref} is the reference dose using the standard phantom.

To verify the local phantom for organ dose measurement, bovine tissues (i.e., eye, esophagus, brain, thyroid, heart, kidney, lung, and liver) were placed in the inserts of the phantoms as shown in Figure 3. The set up was CT-scanned and the HUs for each organ were obtained from the CT console (Figure 4). The obtained HUs were then compared to those of corresponding human tissues reported in the literature.

Statistical analysis

The data analysis was performed using SPSS for Windows, Version 16.0 (SSPSS Inc., Chicago, IL, USA). Descriptive and independent sample t-test was used at a 95% level of significance. $P < 0.05$ was considered statistically significant.

Results

The mean dose obtained from the TLDs for the local CT head phantom was 24.29 mGy, while that of the standard head phantom was 28.28 mGy, showing a percentage difference of 15.2%. Independent samples *t*-test reflected no significant difference in dose value between the local and standard head phantoms ($P=0.060$) and local and standard body phantoms ($P=0.795$), as shown in Table 2. The mean dose of the local CT body phantom was 7.30 mGy, while that of the standard body phantom was 6.92 mGy, revealing a percentage difference of 5.3% as shown in Table 3. Variation in TLD readout may be due to insert orientation, moisture, or temperature. As seen in Table 4, the $CTDI_{vol}$ for the local CT head phantom (47.50 mGy) was lower than that of the standard head phantom (57.93 mGy), with a percentage difference of 19.8%. Also, the $CTDI_{vol}$ for the local CT body phantom (12.05 mGy) was lower than that of the standard body phantom (14.39 mGy) with a percentage difference of 17.7%.

Table 5 shows the results for the verification of the HUs of bovine tissues as obtained from the CT console. There were no significant differences in HU between the bovine and human brain, kidney, liver, and lung tissues ($P=0.938$).
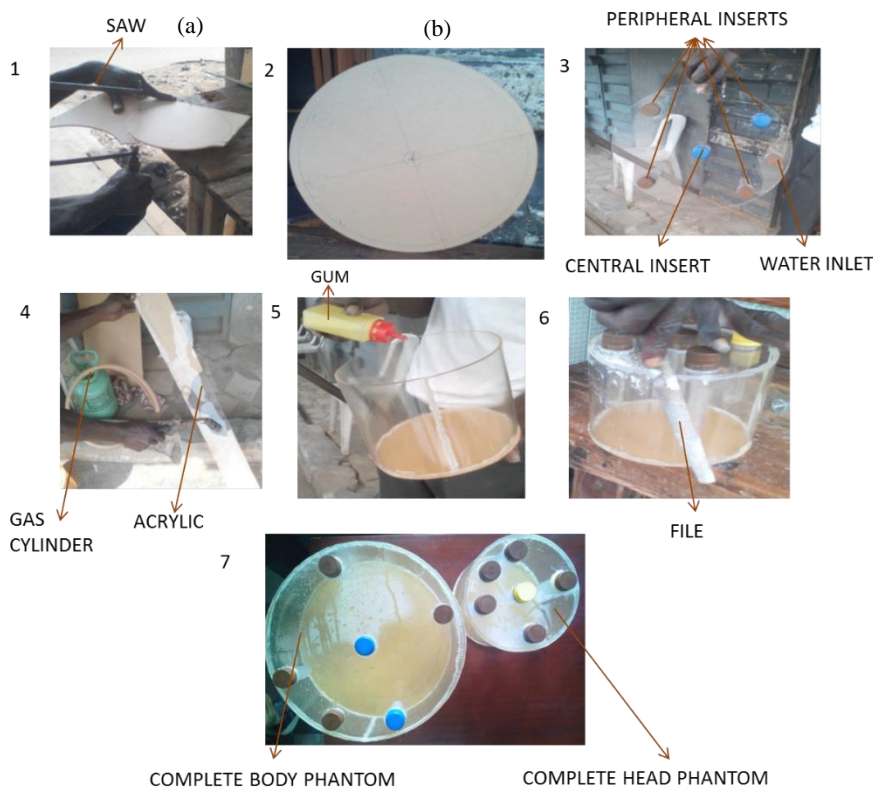

Figure 1. Stages of development and completion of the local phantoms

Table 1. The scan parameters used for the head and body phantoms (local and standard)

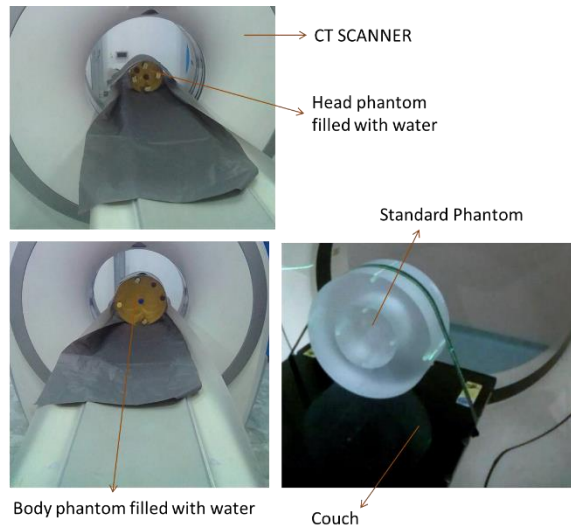| CT scan parameter	Head	Body
kVp	120	100
mA	220	230
Eff. mA	258	115
Rotation time (s)	0.75	0.5
Slice thickness (mm)	5	5
Scanning range (mm)	200	298
Scan length	200	298
Mode	Helical	Helical
Pitch	1	1
Field of view	220.31	366.40
Beam collimation (mm)	10	5
Number of scan series	1	1
Beam width	10	5

Figure 2. Experimental setup for the validation of local body phantoms against standard phantoms
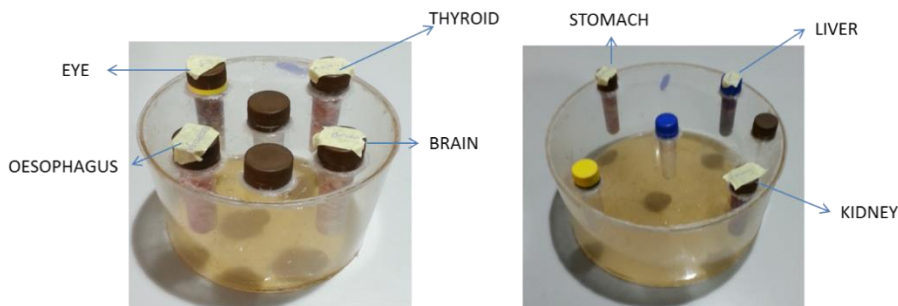

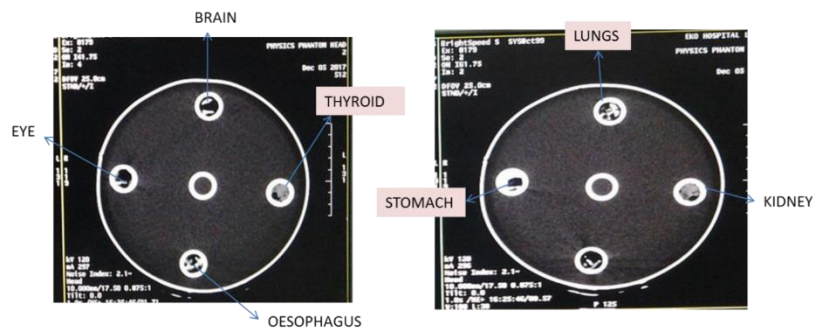**Figure 3**. The developed phantoms with the bovine tissues in position

Figure 4. Computed-tomography scans of the phantoms containing the bovine tissues

Table 2. Thermoluminescent dosimeter readings for the computed-tomography head phantoms (standard and local)

Phantom	Radiation dosage (mGy)?			Mean (mGy)	SD	CV (%)	PD (%)
	Reading 1	Reading 2	Reading 3				
Local head	26.58	24.23	22.06	24.29	2.26	9	15.2
Standard head	30.80	28.72	25.32	28.28	2.76	30	15.2

SD =Standard Deviation, CV(%)= Coefficient of Variance, PD (%)= Percentage Difference

Table 3. Thermoluminescent dosimeter readings for the computed-tomography body phantoms (local and standard)

Protocol	Radiation dosage (mGy)			Mean (mGy)	SD	CV (%)	PD (%)
	Reading 1	Reading 2	Reading 3				
Local body	6.40	7.15	8.34	7.30	0.98	13	5.3
Standard body	6.20	5.27	9.30	6.92	2.11	30	5.3

SD = Standard Deviation, CV(%)= Coefficient of Variance, PD (%)= Percentage difference

Table 4. Dose parameters for the computed-tomography phantoms

Dose parameter	Local head	Standard head	Local body	Standard body
$CTDI_{vol}$(mGy)	47.50	57.93	12.05	14.39
Dose length product (mGy.cm)	1146.20	980.83	348.00	327.96

$CTDI_{vol}$: Weighted computed-tomography dose index

Table 5. The Hounsfield unit of bovine tissues compared to human tissues

Matter	Bovine tissues (HU)	Human tissues (HU)
Brain	31.67 ± 0.58	$20 - 45$
Eye	97.00 ± 3.61	-
Stomach	-127.78 ± 25.56	-
Kidney	76.47 ± 10.86	$20 - 45$
Liver	-78.47 ± 118.67	60 ± 6
Lungs	-657.6 ± 95.7	$(-700) - (-600)$
Heart	-57.6 ± 69.5	-
Water	0	0
Esophagus	40.0 ± 30.5	-
Thyroid	57.4 ± 18.3	-

Discussion

TLD dose measurement is a simplified accurate technique for the dose range from 0.5 cGy to 1000 cGy [16]. The mean TLD readout (Table 2) for the local CT head phantom (24.29 mGy) was lower than that of the standard phantom (28.28 mGy), but it was comparable to the TLD readout of the standard head phantom with the same coefficient of variance (9%) and percentage difference of 15.2%. However, this difference was within the acceptable limit of ±20% [11]. Since the TLD readouts (local and standard) were within the standard limits, it validates that the local head phantom is suitable for dosimetry and CT calibration.

The mean dose (Table 3) for the local CT body phantom (7.30 mGy) was higher than that for the standard phantom (6.92 mGy), with a percentage difference of 5.3%. Nevertheless, this difference was within an acceptable limit of ±20%. This also makes the local CT body phantom suitable for organ dosimetry.

From the results of the local CT phantoms (head and body) and the standard phantoms (tables 2 and 3), it was evident that the doses to the head phantoms (local and standard) were higher than those to the body phantoms (local and standard). For the same kVp and mAs, the radiation doses to smaller phantoms were much greater than those for larger sizes [17]. The percentage difference in the $CTDI_{vol}$ between the standard head phantom (57.93 mGy) and the local head phantom (47.5 mGy) was 19.8%. Nevertheless, variation was within an acceptable margin of ±20%. The results were found to be consistent with the reported values for CTDI by AAPM (49.6 mGy) [11], Hasford (42.40 mGy) [14,18,19], and Aweda et al. (40 mGy) [3]. Our results also met the American College of Radiology (ACR) CT accreditation requirement that the $CTDI_{vol}$ should be within the range of 40-60 mGy for the adult head protocol [4].

The estimated CTDI_vol measurement from a standard body phantom is used as a reference for a normal adult torso phantom, which includes the chest, abdomen, and pelvis and is similar to a pediatric body phantom for some CT manufacturers [20]. The estimated CTDI_vol for the local body phantom (12.05 mGy) was compared to the $CTDI_{vol}$ for the standard phantom (14.39), and a percentage difference of 17.7% was obtained. This result was consistent with the values reported by AAPM 1992 [11] (27.8 mGy), Hasford (19.49 mGy) [14], and Aweda et al. (12 mGy) [3]. The result meets the ACR CT accreditation requirement that the $CTDI_{vol}$ should be within the range of 10-40 mGy for the adult body protocol [4]. Our findings support the findings of Aweda (2007) and are within the ACR range.

In general, CTDI appears to be an exponential function of phantom diameter, kVp, and mA. The radiation doses for small phantoms with the same KVp and mA values are greater than those for large-sized phantoms [17, 21], which means that doses to the organs in the head are twice as high as those to the organs in the body using the same technique. The mean HU of bovine brain tissue (31.67±0.58; Table 4) was in concord with that of normal human brain tissue, which is within the range of 20–45. For kidneys, the HU for bovine tissue (76.47±10.86) was greater than that of human tissue (20-45), which may be due to spaces in the tissues within the inserts.

The mean HU for bovine liver tissue was -64.47±118.67 (54.2), and for the human tissue it was 60±6, which are in agreement. Regarding the lungs, the mean HU for bovine tissue was -657.6±95.7 (-561.9 or -753.3), and the range for human tissue was -700 to -600. In our study, the HU for human lung tissue, which is much lower than that of Bagdare et al. [22], is in line with the average standard for a normal person. Other organs and their mean HUs include esophagus (40.0±30.5), thyroid (57.4±18.3), and eye lens (97.00±3.61). These values are lower in comparison with the findings of Ernst et al. [23], where TLD-100 LiF detectors placed at 71 measurement positions were assessed in the head and neck regions, and that of Pi Y et al. [24], where the radiation dosage to 120 organs/tissues samples where obtained. HU variation or accuracy may be affected by scanner type, convolution kernel, reconstruction artifacts, beam hardening, spectral energy, as well as variation in patient size (phantom size) and phantom shape and position (patients) in the scanner [25, 26]. Our study was limited to organ types and did not include various samples, which can account for the limited organ tissues in the phantoms unlike the studies performed among the Chinese population, where they could correct for age and gender [24, 25, 27, 28].

Conclusion

A local CT phantom (head and body) was developed, which was validated with a standard phantom using the same protocol. The CTDI of the local CT phantoms (head and body) and the standard phantoms showed good agreement within ACR ranges. The variation in TLD values could be due to annealing duration, temperature, pressure, long-term radiation exposure, and moisture. Finally, the HUs of the bovine tissues placed in the inserts closely matched those of the corresponding human tissues. The observed variations may be due to spaces between tissues in the inserts and variation in patient size (phantom), shape, and phantom position (patients) in the scanner. Compared to standard head and body phantoms, the designed phantoms showed an overall good accuracy. It will be a useful tool for quality assurance and quality control tests in radiology departments in Nigeria.

References

1. Bushberg JT, Siebert JA, Leidholdt SB, Boone JM. The Essential Physics of Medical Imaging 2nd Ed. Lippincott W, W. NY. 2012.
2. Rehani MM, Berry M. Radiation Doses in Computed Tomography: the Increasing doses of radiation need to be controlled. British Med Jour.2000; 320: 593–4.
3. Aweda MA, Arogundade RA. Patient dose reduction methods in computerized tomography procedures: A review. Int Jour of Phy Scien.2007; 2:1-9
4. Winslow J, Daniel E, Ryan F, Christopher J, David E. Construction of anthropomorphic phantoms for use in dosimetry studies. Jour of appl clinical med Phys. 2009; 10:3.
5. International Atomic Energy Agency. Optimization of the radiological protection of patients undergoing radiography, fluoroscopy and computed tomography. Final report of a coordinated research project in Africa, Asia and Eastern Europe. IAEA-TECDOC. 2004;1423.
6. Cakmak ED, Tuncel N, Sindir B. Assessment of organ dose by direct and indirect measurements for a wide bore x-ray computed tomography unit that used in radiotherapy. International Journal of Medical Physics, Clinical Engineering and Radiation Oncology. 2015; 4(02): 132.
7. Kopp AF, Heuschmid M, Claussen CD. Multidetector helical CT of the liver for tumor detection and characterization. European radiology. 2002; 12(4): 745-52.
8. Toth TL. Dose reduction opportunities for CT scanners. Pediatric radiology. 2002 Apr 1;32(4):261-7.
9. Itoh S, Koyama S, Ikeda M. Further Reduction of Radiation Dose in Helical CT for Lung cancer Screening Using Small Tube Current and a Newly Designed Filter. J. Thorac. Imaging. 2001; 16:81–8.
10. Naseri S, Momen Nezhad M, Hozhabri Z, Haghparast A, Karami G, Hejazi P. Optimization of Parameters in 16-slice CT-scan Protocols for Reduction of the Absorbed Dose. Iranian Journal of Medical Physics. 2014; 11: 270-5.
11. American Association of Physicists in Medicine, Barnes GT, Gould RG, Seibert JA. Specification, acceptance testing and quality control of diagnostic x-ray imaging equipment. American Association of Physicists in Medicine; 1994.
12. Dixon RL, Anderson JA, Bakalyar DM, Boedeker K, Boone J, Cody D. Comprehensive methodology for the evaluation of radiation dose in x-ray computed tomography. Report of AAPM Task Group. 2010; 111: 20740-3846.
13. AAPM. Site specific dose estimates (SSDE) in paediatric and adult body CT examinations. AAPM Report No. 204. Report of AAPM Task Group 204 of AAPM. College Park, MD. 2011.

14. Hasford F, Van Wyk B, Mabhengu T, Vangu MD, Kyere AK, Amuasi JH. Determination of dose delivery accuracy in CT examinations. Journal of Radiation Research and Applied Sciences. 2015; 8(4): 489-92.

15. Leitz W, Axelsson B, Szendrö G. Computed Tomography Dose Assessment - A practical approach to radiation protection dosimetry. Nuc. Tech. Pub. 1995; 57:377-80.

16. Yu C , Luxton G. TLD dose measurement: A simplified accurate technique for the dose range from 0.5 cGy to 1000cGY. Med Phys. 1999; 26(6): 1010-6.

17. Edward LN, Ajoy KD , Zheng FL. Influence of phantom diameter, kVp and scan mode upon computed tomography dose index. International. Journal of medical physics. Radiation protection physics.2003; 30: 395-402.

18. Sinclair L, Griglock TM, Mench A, Lamoureux R, Cormack B, Bidari S. Determining organ doses from CT with direct measurements in postmortem subjects: part 2—correlations with patient-specific parameters. Radiology. 2015; 277(2): 471-6.

19. Mahur M, Gurjar OP, Grover RK, Negi PS, Sharma R, Singh A. Evaluation of Effect of Different Computed Tomography Scanning Protocols on Hounsfield Unit and Its Impact on Dose Calculation by Treatment Planning System. Iranian Journal of Medical Physics. 2017; 14(3): 149-54.

20. Shrimpton P. Assessment of patient dose in CT: European guidelines for multislice computed tomography funded by the European Commission 2004: contract number FIGMCT2000-20078-CT-TIP. Luxembourg, Luxembourg: European Commission. 2004.

21. Huda W, Ogden KM. Comparison of head and body organ doses in CT. Physics in Medicine & Biology. 2007; 53(2): N9.

22. Bagdare PB, Dubey S, Ghosh SK, Gurjar OP, Bhandari V, Gupta KL. A study on slab-wooden dust-slab phantom for the development of thorax phantom. Iranian Journal of Medical Physics. 2018; 15(2): 71-7.

23. Ernst M, Manser P, Dula K, Volken W, Stampanoni MF, Fix MK. TLD measurements and Monte Carlo calculations of head and neck organ and effective doses for cone beam computed tomography using 3D Accuitomo 170. Dentomaxillofacial Radiology. 2017; 46(7): 20170047.

24. Pi Y, Liu T, Xu XG. Development Of A Set Of Mesh-based And Age-dependent Chinese Phantoms And Application For Ct Dose Calculations. Radiation protection dosimetry. 2018; 179(4): 370-82. DOI: 10.1093/rpd/ncx296.

25. Lamba R, McGahan JP, Corwin MT, Li CS, Tran T, Seibert JA. CT Hounsfield numbers of soft tissues on unenhanced abdominal CT scans: variability between two different manufacturers' MDCT scanners. American Journal of Roentgenology. 2014; 203(5): 1013-20.

26. Nazarnejad M, Mahdavi SR, Asnaashari K, Sadeghi M, Nikoofar A. Developing a verification and training phantom for gynecological brachytherapy system. Iranian Journal of Medical Physics. 2012; 9(1): 33-40.

27. Kamaruddin N, Rajion ZA, Yusof A, Aziz ME. Relationship between Hounsfield unit in CT scan and gray scale in CBCT. InAIP Conference Proceedings. 2016 ; 1791: 1.

28. Razi T, Niknami M, Ghazani FA. Relationship between Hounsfield unit in CT scan and gray scale in CBCT. Journal of dental research, dental clinics, dental prospects. 2014; 8(2): 107.